Leila Lamiri* and Belkacem Nessark

Electrochemical behavior, characterization and corrosion protection properties of poly(bithiophene + 2-methylfuran) copolymer coatings on A304 stainless steel

https://doi.org/10.1515/epoly-2017-0057
Received March 23, 2017; accepted July 24, 2017; previously published online September 19, 2017

Abstract: Polybithiophene (PBTh), poly(2-methylfuran) (PMeFu) and poly(bithiophene + 2-methylfuran) noted poly(BTh + MeFu) copolymer films were synthesized by electrochemical deposition on 304-stainless steel, from an acetonitrile (ACN) solution containing 10^{-2} M bithiophene, 10^{-2} M 2-methylfuran and 10^{-1} M lithium perchlorate ($LiClO_4$), by cyclic voltammetry (CV) between 0 V and 2 V vs. SCE, with a scan rate of 50 mV · s^{-1}. The copolymers coated were studied in a corrosive sulfuric acid medium (H_2SO_4 · 1 N) using the potensiodynamique polarization method and the electrochemical impedance spectroscopy (EIS). Copolymers coated characterization was performed using scanning electron microscopy (SEM) and Fourier transform infrared (FTIR) spectroscopy. The polarization curves show that the copolymer film formed on A304, shifts the corrosion potential towards more positive potentials. The presence of the poly(BTh + MeFu) improves the corrosion resistance of the metal in a corrosive medium, H_2SO_4. This protection against corrosion is caused by the barrier effect of the layer of copolymer, which covers the surface of the A304 stainless steel against the aggressive ions of the corrosive medium.

Keywords: 2-methylfuran; bithiophene; copolymers; protection against corrosion; stainless steel.

1 Introduction

The majority of the well-known inhibitors are organic compounds containing heteroatoms, such as oxygen (O), nitrogen (N) or sulfur (S), which allow adsorption on the metal surface (1). Many studies are interested in polyheteroaromatics because of their common use in a wide range of industrial applications including electrochromic devices (2), photovoltaic cells (3) and corrosion protection (4). Among the many profuse applications of conjugated polymers the use of corrosion inhibitors is probably the most attractive from the point of view of economics and ease of application (5).

Conducting polymers that are either chemically or electrochemically deposited on the metal substrate have now been used as corrosion protection coatings (6). Electroactive polymer films also exhibit an effective physical barrier property against aggressive species (such as O_2, H^+ and Cl^-) and provide anodic protection to metals, under various conditions (7). Conducting polymers have been evaluated for their corrosion protection of mild steel, stainless steel, iron, copper, zinc, aluminum and other metals (8), several organic compounds have been evaluated as inhibitors for the corrosion of A304 stainless steel in an acid medium (9) and the passivation of stainless steels by chemically or electrochemically coating with conductive polymer has been studied (10).

Among the family of conducting polymers, polythiophene (PTh), polyfuran (PFu) and their derivatives have been employed for advanced anticorrosion protection, Tüken et al. (11) showed in 2004, that the polythiophene film had a great corrosion resistance performance. Ren and Barkey (12) achieved the synthesis of poly(3-methyl thiophene) films on 430 stainless steel in a nonaqueous medium galvanostatically and showed that the film protected the substrate efficiently in 0.5 M sulfuric acid. Whereas, Refaey et al. (13) protected mild steel using formation of polybithiophene film on its surface. In another study using poly(3-octylthiophene) and poly(3-hexylthiophene) on 1018 carbon steel to protect it against corrosion in 0.5 M H_2SO_4 and poly(3-octylthiophene) in 0.5 M NaOH have been investigated as protective coatings against corrosion of metals (14, 15). However, polybithiophene (PBTh) coatings on stainless steel for the prevention of corrosion behavior have been synthesized using the electrochemical method (16, 17).

***Corresponding author: Leila Lamiri,** Laboratoire d'Electrochimie et Matériaux, Département de Génie des Procédés, Faculté de Technologie, Université Ferhat Abbas Sétif-1, 19000 Sétif, Algérie; and Research Center in Industrial Technologies CRTI, P.O. Box 64, Cheraga 16014, Algiers, Algeria, e-mail: lamiri.lila@yahoo.fr
Belkacem Nessark: Laboratoire d'Electrochimie et Matériaux, Département de Génie des Procédés, Faculté de Technologie, Université Ferhat Abbas Sétif-1, 19000 Sétif, Algérie

Many studies have used the corrosion protection of copolymers such as aniline with pyrrole (18), pyrrole with N-methyl pyrrole (19), pyrrole with bithiophene (20). Some groups have chosen furan to copolymerize with thiophene (21), 3-methylthiophene (22).

In this study, PBTh, PMeFu and poly(BTh + MeFu) copolymer, were synthesized using cyclic voltammetry (cycling), in acetonitrile solution containing correspondent monomers. The use of these copolymers as corrosion protection coatings on stainless steel (A304) was carried out in the corrosive medium of H_2SO_4 1 N, using potentiodynamic polarization and impedance spectroscopy (EIS) techniques. The morphology of the modified metal surface was characterized by using scanning electron microscopy (SEM) and Fourier transform infrared (FTIR) spectroscopy.

2 Experimental section

The monomers used are bithiophene and 2-methylfuran, (Aldrich, USA). Their chemical structures are shows in Scheme 1. The supporting electrolyte used was lithium perchlorate ($LiClO_4$) (Fluka, Switzerland) in the acetonitrile solvent CH_3CN (Aldrich), which is a pure salt suitable for analysis purposes. This electrolyte was chosen because of its solubility in organic and aqueous solutions and because of its electrochemical stability on a large domain of potential.

The electrochemical polymerization of BTh and MeFu was performed by cyclic voltammetry sweeping in the potential range between 0 V and 2 V vs. SCE, at a scan rate of 50 $mV \cdot s^{-1}$ in $CH_3CN/LiClO_4$ 10^{-1} M containing the bithiophene or 2-methylfuran or the two monomers at the same time.

The cell used for electrochemical measurements was a typical three-electrode connected with a potentiostat/galvanostat model PGZ 401 Voltalab system, the working electrode was stainless steel (A304) disk (Ø = 2 mm), the counter electrode is a platinum wire, and a saturated calomel electrode (SCE) was used as a reference electrode.

The obtained modified electrodes: PBTh/A304, PMeFu/A304 and poly(BTh + MeFu)/A304 were studied in aggressive sulfuric acid (H_2SO_4 1 N) medium. The polarization study was carried out from –1.2 V to 2 V vs. SCE, at scan rate 50 $mV \cdot s^{-1}$. The working electrode was immersed in a test solution for 30 min to establish a steady state open circuit. The potentiodynamic polarization curves obtained by linear extrapolation of the anodic and cathodic branches of the Tafel plots. Electrochemical impedance (EIS) measurements were carried in the frequency range of 100 kHz–100 mHz after an immersion time of 30 min in the acidic medium (H_2SO_4 1 N).

The surface morphologies of A304, and A304 modified by PBTh, PMeFu and poly(BTh + MeFu) were collected using scanning electron microscopy (SEM, JOEL-JSM-7001F). FTIR spectra of the copolymer were taken using a Shimadzu 8101 M spectrophotometer between 4000 and 400 cm^{-1}.

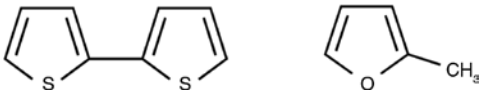

Scheme 1: Chemical structure of bithiophene (BTh) and 2-methylfuran (MeFu).

3 Results and discussion

3.1 Electropolymerization of bithiophene on A304 stainless steel

The successive cyclic voltamperograms relative to bithiophene 10^{-2} M in $CH_3CN/LiClO_4$ (10^{-1} M), on an A304 stainless steel electrode, recorded between the potential range 0 and 2 V/SCE, with a scan rate of 50 $mV \cdot s^{-1}$ are shown in Figure 1.

It is observed that during the positive potential sweep, a shoulder which appears only in the first cycle at 1.32 V vs. SCE and a second at 1.65 V vs. SCE, are attributed,

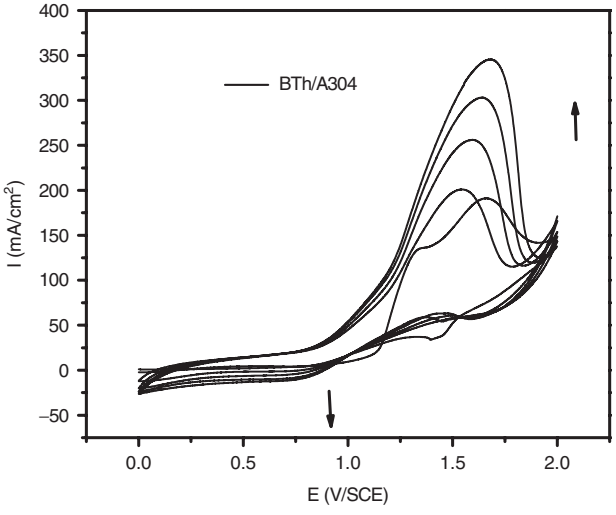

Figure 1: Cyclic voltammograms (cycling) corresponding to the bithiophene 10^{-2} M in $CH_3CN/LiClO_4$ (10^{-1} M) solution, recorded between 0 V and 2 V vs. SCE, at a scan rate of 50 $mV \cdot s^{-1}$, on an A304 electrode (Ø = 2 mm).

respectively, to the first and second oxidation of BTh. During the negative potential scan, a cathodic peak was observed around 0.75 V vs. SCE preceded by a shoulder at 1.41 vs. SCE which disappears during the successive scanning of the potential, corresponding to the reduction of the formed polymer film PBTh/A304. After the second cycle, the vague and peak sets are observed as a single intensive peak around 1.55 V vs. SCE.

The intensity of the latter increases during the cycling. This indicates that the polymer is in the process of settling on the A304 electrode, which is covered completely by a film of PBTh. This kinetic behavior has previously been observed by the work Nessark et al. (23) when they filed the terthiophen on 304-stainless steel. The polymer film is accompanied by a reversible change in color that changes from red brick during oxidation to blue night during the reduction.

3.2 Electropolymerization of 2-methylfuran on A304 stainless steel

Figure 2 shows the cyclic voltammograms of MeFu in a $CH_3CN/LiClO_4$ solution (10^{-1} M) recorded between 0 V and 2 V vs. SCE, at a scan rate of 50 $mV \cdot s^{-1}$.

The voltammogram shows an anodic wave at 1.54 V vs. SCE in positive scan potential, this is characteristic of MeFu monomer oxidation. This wave disappeared after the second cycle when a film of PMeFu was obtained on the electrode, and a low current was observed from the second cycle. This shows that the PMeFu plays an important role and the kinetics help protect the metal against corrosion, as was shown with other studies (24). The negative cathodic scan peak at 0.64 V vs. SCE was attributed to the reduction of PMeFu/A304. A slight decrease of the current intensities of the anodic and cathodic peaks was observed. This is probably due to the inhibition of the surface by an insulating polymeric film which was carried out on the electrode. Nessark et al. (25) also suggested that the current intensity of the anodic peak decreases during cycling and it stabilizes after many cycles when the electrode surface is coated by an insulating film.

3.3 Electropolymerization of (bithiophene + 2-methylfuran) copolymer

Figure 3 represents the cyclic voltammograms relative to an A304 steel electrode in $CH_3CN/LiClO_4$ (10^{-1} M) solution, containing BTh (10^{-2} M) and MeFu for different concentrations (10^{-4}, 10^{-3} and 10^{-2} M), which were obtained at a scan rate recording at $v = 50\ mV \cdot s^{-1}$, between 0 V and 2 V vs. SCE.

The obtained cyclic voltammograms during the positive scan potential, show an anodic peak at 1.35 V followed by a shoulder at 1.46 V vs. SCE which are characteristic for the oxidation of the two monomers (bithiophene and 2-methylfuran) present in the solution. During cathodic scan potential, there was a peak at 0.72 V vs. SCE corresponding to the reduction of the copolymer.

It is also shown that there was a slight decrease of the current intensities of the anodic and cathodic peaks.

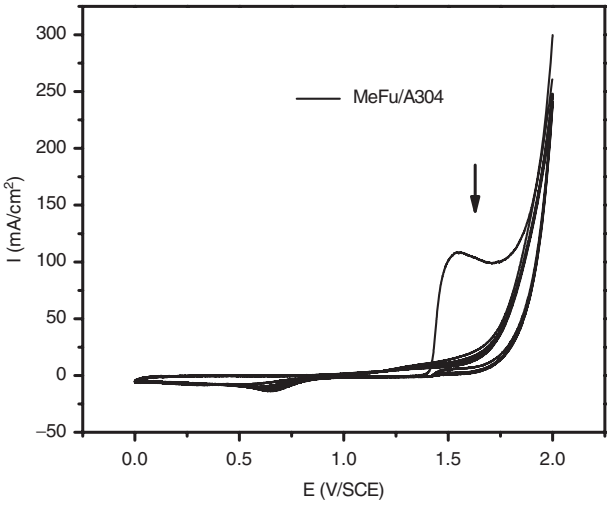

Figure 2: Cyclic voltammograms (cycling) corresponding to the 2-methylfuran 10^{-2} M in $CH_3CN/LiClO_4$ (10^{-1} M) solution, recorded between 0 V and 2 V vs. SCE, at a scan rate of 50 $mV \cdot s^{-1}$, on an A304 electrode (Ø = 2 mm).

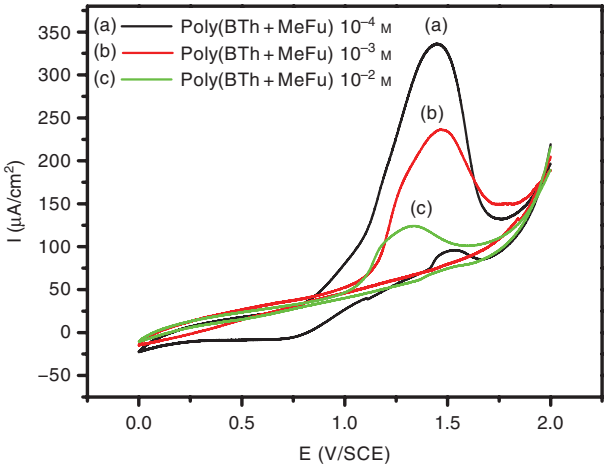

Figure 3: Cyclic voltammograms relating to a solution of bithiophene 10^{-2} M dissolved in $CH_3CN/LiClO_4$ (10^{-1} M), obtained for different concentrations of MeFu [(a) 10^{-4}, (b) 10^{-3} and (c) 10^{-2} M], recorded at $v = 50\ mV \cdot s^{-1}$, between –1.2 V and 2 V vs. SCE, on an A304 electrode (superposition of the first cycles).

This is accompanied by a slight shift of the anodic peak potential towards less positive values and the cathodic peak towards more negative values, with an increase in MeFu concentration. This suggests that the presence of the latter inhibits the electropolymerization reaction of bithiophen and contributes to the formation of a less conducting film. A similar behavior was observed on a platinum electrode (26).

3.4 Potentiodynamic polarization curves

Although the Tafel extrapolation method is usually insufficient to understand the protective properties of organic polymer coatings drivers, this method can be used to compare corrosion performances of various types of coating polymers (27).

In this part we examine the evolution of electrochemical parameters of A304, PBTh film in the absence and presence of various concentrations of 2-methylfuran. Before each immersion, A304 electrode was cleaned by polishing with sand paper. Then it was rinsed with distilled water. The Tafel curves were recorded at a scan rate of 50 mV · s^{-1}, the film was analyzed in a corrosive medium (H_2O/H_2SO_4 1 N) after immersion for 30 min.

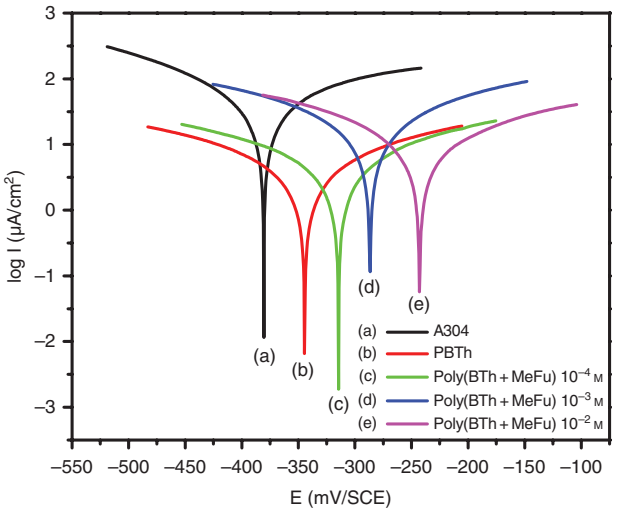

Figure 4: Tafel curves corresponding to the electrode modified poly(BTh + MeFu)/A304 in a solution of H_2O/H_2SO_4 1 N.

Figure 4 shows the Tafel curves corresponding to A304 with and without a coating of the copolymer being studied. The electrochemical parameters such as corrosion potential (E_{corr}), corrosion current density (i_{corr}), anodic and cathodic Tafel slopes (b_a and b_c), polarization resistance (R_p) values and protection efficiencies (η_p) are summarized in Table 1. The percentage protection efficiencies (η_p) of coating were calculated using the relationship:

$$\eta_p\,\% = \frac{i^0_{corr} - i_{corr}}{i^0_{corr}} \times 100$$

where i^0_{corr} and i_{corr} are the corrosion current densities of uncoated and coated electrodes.

We see that E_{corr} values increased from –380.4 mV (A304) to –344.4 mV (PBTh/A304) it increases with an increase in the concentration of MeFu and these values were –314.5, –286.7 and –242.8 mV, respectively. It moves toward more positive values (20). On the other hand, the values of the i_{corr} decrease with the addition of MeFu, initially. However, the value of this current begins to increase after from the second concentration 10^{-4} M (see third curve), while remaining less than that observed for the metal alone. In light of these results we can say that films of poly(BTh + MeFu) improve the corrosion resistance of steel in H_2SO_4 1 N medium. Rajendran et al. (28) have reported similar behavior of poly(N-(methacryloyloxymethyl)benzotriazole-coglycidylmethacrylate) coatings on mild steel in 0.1 M HCl. We note here that the increase of the corrosion potential towards more positive values, accompanied by an increase in the corrosion current from the third curve, result in the modification of the physicochemical properties of the film (nature of the film, real surface), which vary as 2-methylfuran is added in the solution. Thus, the current in no way could be read as a current of corrosion of the metal alone, but it is a current of the whole (stainless steel and copolymer).

Table 1: Parameters of the steel from corrosion A304 modified by PBTh and copolymer poly(BTh + MeFu) for different concentrations.

	E_{corr} (mV/SCE)	R_p (kΩ · cm²)	i_{corr} (µA/cm²)	b_a (mv/dec)	b_c (mv/dec)	η_p (%)
A304/H_2SO_4 1 N	–380.4	709	36.61	188.9	–133.5	/
PBTh	–344.4	7.6	5.18	240.9	–246.8	85.85
PBTh + MeFu 10^{-4} M	–314.5	6.81	5.20	203.2	–230.6	85.79
PBTh + MeFu 10^{-3} M	–286.7	1.73	5.74	248.5	–273.4	84.32
PBTh + MeFu 10^{-2} M	–242.8	2.84	12.99	277.9	–207.5	64.71

3.5 Electrochemical impedance measurements (EIS)

The impedance measurement is a widespread method in the anti-corrosion coating processes (29) and an *in situ* method for characterizing polymer coated metal and changes in their performance during exposure in corrosive environments (30).

Figure 5 shows the Nyquist plots of A304 and poly(BTh + MeFu)/A304 electrodes obtained for different concentrations of MeFu immersed in a sulfuric medium (H_2O/H_2SO_4 1 N). As shown the impedance diagrams obtained are complex and they consist of a large capacitive loop in the high frequencies region followed by a small inductive loop at low frequencies.

The capacitive loop observed at high frequencies, is characteristic of the charge transfer resistance (R_{ct}) of the corrosion process and the double layer capacitance (C_{dl}) of the liquid/metal interface (31, 32). In the literature, the low frequencies inductive loop is assigned to the relaxation process of the film that is coated on the surface of the electrode (33, 34). The diameter of the capacitive loop of (BTh+MeFu) copolymer increases with the increase in MeFu concentration suggesting an augmentation in the charge transfer resistance (R_{ct}) and thus a decrease of the double layer capacitance (C_{dl}) of (BTh+MeFu) copolymer film, which indicates a decrease in the porosity of the film and a barrier effect of the performance improvement for the protection against corrosion of the steel substrate (35).

Figure 6 shows the assumed equivalent circuit. The equivalent circuit presented in Figure 6 refers to the work of Yuan et al. (36). The impedance behavior of the uncoated electrode can be represented by the equivalent circuit shown in Figure 6A, where R_Ω is the electrolyte resistance, the conventional double-layer capacitance is replaced by a constant phase element (CPE) in order to give a more accurate fit to the experimental results (37) at high frequency and the Warburg diffusion impedance (W) at low frequency.

As can be seen in Figure 6B, the correspondent circuit model of poly(BTh + MeFu) coated electrode, this is the most frequent circuit model used to describe the corrosion mechanism of metal/polymer electrodes (38). In this circuit (Figure 6B), C_{dl} is the double layer capacitance, R_{ct} the interfacial charge-transfer resistance, L the inductance and R_L the inductive resistance (39).

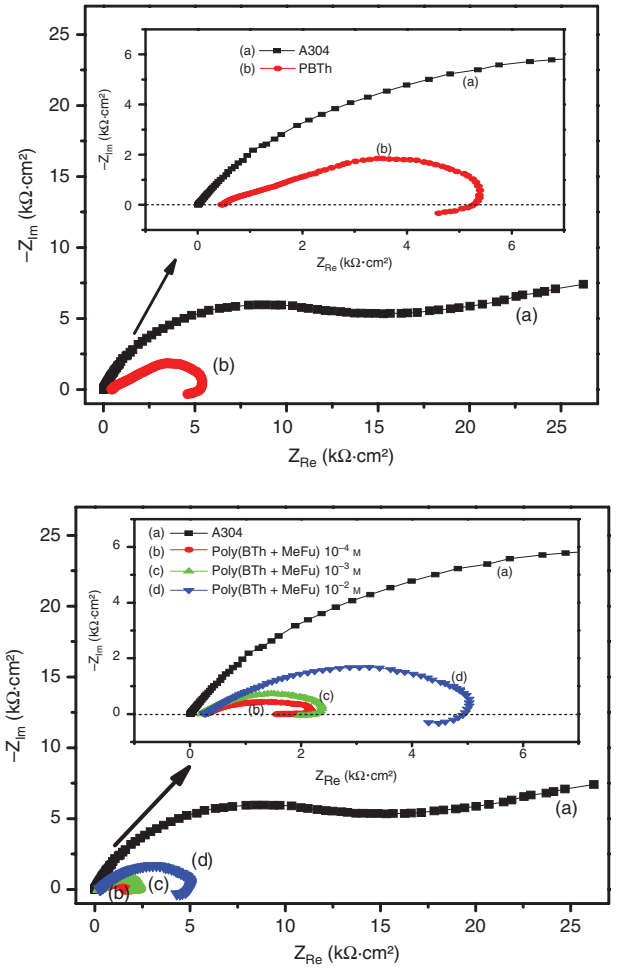

Figure 5: Nyquist diagrams corresponding to poly(BTh + MeFu)/A304 in (H_2SO_4 1 N) obtained on a frequency range between 100 kHz and 100 mHz.

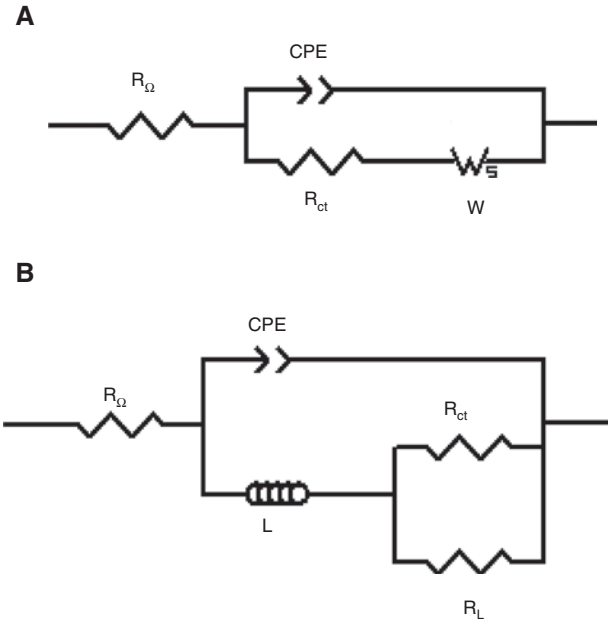

Figure 6: Equivalent circuit of: uncoated electrode A304 (A), and coated electrode poly(BTh + MeFu)/A304 (B).

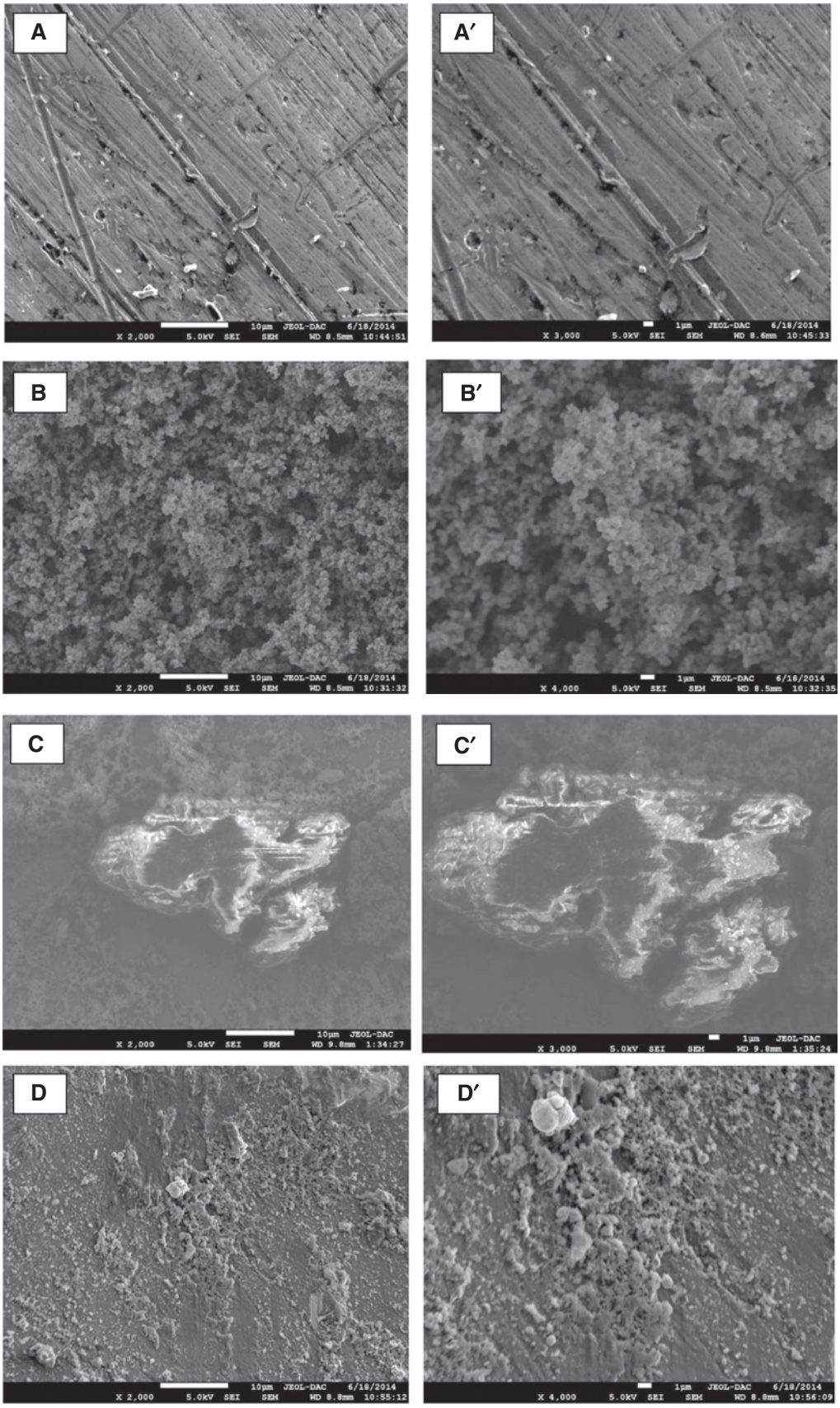

Figure 7: SEM images of (A, A′) A304, (B, B′) PBTh/A304, (C, C′) PMeFu/A304 and (D, D′) copolymer (scale bar: 10 μm and 1 μm).

3.6 Scanning electron microscopic (SEM) analyses

SEM images are shown in Figure 7. The single A304 steel surface is polished before being exposed to the aggressive environment and where the polishing lines of the surface of the steel are visible (40). The microstructures of the surfaces in the presence of the PBTh film clearly show that the morphology of PBTh on steel has a porous, spongy structure (Figure 7A,A′), a similar behavior was observed for the polyterthiophene coated A304 (23). Concerning the PMeFu, the coating surface presents higher porosity and the film formed is very thin (transparent), suggesting that the latter partially covers the surface of the substrate (Figure 7B,B′). In some cases, acceleration of corrosion was also noticed due to the presence of micropores in the electrodeposed PMeFu coating (24).

The morphology of poly(BTh + MeFu) copolymer (Figure 7C,C′) reveals that the film is formed by granules of the both polymers, this resulted in a reduced rate of corrosion and a higher corrosion protection performance of the coating on the metal substrate.

3.7 Fourier transforms infrared spectroscopy (FTIR)

FTIR spectra of PBTh and PMeFu and poly(BTh + MeFu) copolymer recorded in the wave number range 400–4000 cm^{-1} are presented in Figure 8.

For the spectrum of the PBTh, the absorption band located at 790 cm^{-1} is due to the stretching vibration of the C-S-C bond (41), the band at 1600 cm^{-1} belongs to C=C stretching modes of vibrations in the thiophene ring (42). The band at 1085 cm^{-1} represents the C-H ring breathing (43). The band near 1350 cm^{-1} is probably due to a stretching vibration of C-C bonds (44). The bands in the region 2810–2970 cm^{-1} are possibly due to the symmetric and asymmetric stretch of methyl groups (44). The absorption bands in the region 2300–2400 cm^{-1} are assigned to the C=C stretching mode and prove the presence of polyconjugation in polybithiophene molecules (44).

In addition, the weak absorption around 1640 cm^{-1} corresponding to the C=O stretching vibration shows that some defects do exist in the polymer film. The presence of this band probably indicates the ring opening of 2-methyl furan with the consequent generation of unconjugated structures (25) such as a 2-methylfuran ring break which was also noted by Carrillo et al. (45).

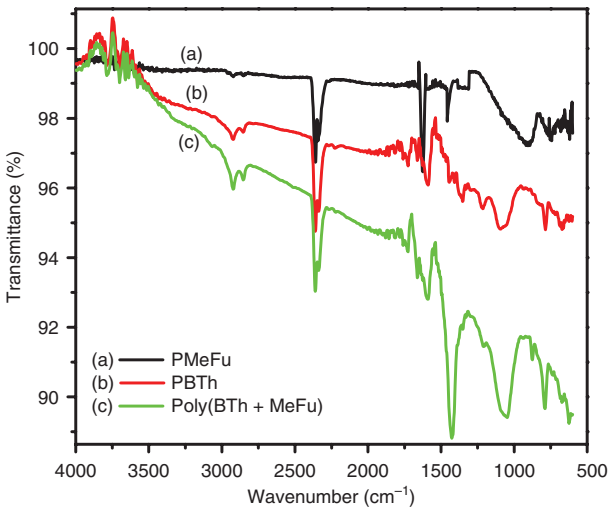

Figure 8: FT-IR absorption spectra of the: (a) PMeFu, (b) PBTh and (c) poly(BTh + MeFu) copolymer.

The band located around 905 cm^{-1} is assigned to C-O stretching vibration. However, the P(BTh + MeFu) copolymer spectrum is almost similar to those of PBTh, the absorption band of the C=C bond in the P(BTh + MeFu) copolymer appears in 1600 cm^{-1}. The slight low-intensity peak at 3060 cm^{-1} can be ascribed to the aromatic C-H stretching vibrations (46). Furthermore, the bands at 795 cm^{-1} indicates that α-α′ coupling of the radical cations has taken place in the copolymerization. This is a characteristic of α-substituted five-membered heterocyclic compounds (47).

4 Conclusion

Poly(BTh + MeFu) copolymer has been successfully electrodeposited on A304 using the cyclic voltammetry technique from bithiophene and 2-methylfuran dissolved in an acetonitrile/$LiClO_4$ solvent/supporting electrolyte system. The performance of the protection of the coating on steel is carried out using the sulfuric acid medium, and characterized by electrochemical impedance spectroscopy (EIS) and Tafel polarization measurements.

The coated poly(BTh + MeFu) copolymer films shift the electrode potential toward more positive values. This results from a modification of the physicochemical properties of the film (nature of the film, real surface), which vary as 2-methylfuran is added in the solution. We noticed that the presence of PMeFu coatings afforded the best protection due to the formation of a coating layer on the metallic surface which behaved like a physical barrier against the aggressive medium attack.

References

1. Machnikova E, Kenton Whitmire H, Hackerman N. Corrosion inhibition of carbon steel in hydrochloric acid by furan derivatives. Electrochim Acta. 2008;53(20):6024–32.
2. Yin B, Jiang C, Wang Y, La M, Liu P, Deng W. Synthesis and electrochromic properties of oligothiophene derivatives. Synth Met. 2010;160(5–6):432–5.
3. Lim E, Lee S, Lee KK, Kang IN, Moon SJ, Kong HY, Katz HE. Solution processable oligothiophenes with solubilizing β-alkyl groups for organic photovoltaic cells. Sol Energ Mater Sol Cells. 2012;107:165–74.
4. Benchikh A, Aitout R, Makhloufi L, Benhaddad L, Saidani B. Soluble conducting poly(aniline-co-orthotoluidine) copolymer as corrosion inhibitor for carbon steel in 3% NaCl. Desalination 2009;249(2):466–74.
5. Ameer MA, Fekry AM. Inhibition effect of newly synthesized heterocyclic organic molecules on corrosion of steel in alkaline medium containing chloride. Int J Hydrogen Energy. 2010;35(20):11387–96.
6. Madhankumar A, Rajendran NA. Promising copolymer of p-phenylendiamine and o-aminophenol: chemical and electrochemical synthesis, characterization and its corrosion protection aspect on mild steel. Synth Met. 2012;162(1–2):176–85.
7. Tüken T, Yazici B, Erbil M. Electrochemical synthesis of polythiophene on nickel coated mild steel and corrosion performance. Appl Surf Sci. 2005;239(3–4):398–409.
8. Riaz U, Nwaoha C, Ashraf SM. Recent advances in corrosion protective composite coatings based on conducting polymers and natural resource derived polymers. Prog Org Coat. 2014;77(4):743–56.
9. Galal A, Atta NF, Al-Hassan MHS. Effect of some thiophene derivatives on the electrochemical behavior of AISI 316 austenitic stainless steel in acidic solutions containing chloride ions I. Effect of temperature and surface studies. Mater Chem Phys. 2005;89(1):38–48.
10. Hermas AA, Nakayama M, Ogura K. Formation of stable passive film on stainless steel by electrochemical deposition of polypyrrole. Electrochim Acta. 2005;50(18):3640–7.
11. Tüken T, Yazici B, Erbil M. The use of polythiophene for mild steel protection. Prog Org Coat. 2004;51(3):205–12.
12. Ren S, Barkey D. Electrochemically prepared poly 3-methylthiophene films for passivation of 430 stainless steel. J Electrochem Soc. 1992;139(4):1021–6.
13. Refaey SAM, Taha F, Shehata HS. Corrosion protection of mild steel by formation of iron oxide polybithiophene composite films. J Appl Electrochem. 2005;34(9):891–7.
14. Medrano-Vaca MG, Gonzalez-Rodriguez JG, Nicho ME, Salinas-Bravo VM. Corrosion protection of carbon steel by thin films of poly (3-alkyl thiophenes) in 0.5 M H_2SO_4. Electrochim Acta. 2008;53(9):3500–7.
15. Leon-Silva U, Gonzalez-Rodriguez JG, Nicho ME, Salinas-Bravo VM, Chacon Nava JG, Martinez-Villafañe A. Effect of thermal annealing on the corrosion protection of stainless steel by poly 3-octyl thiophene. Corros Sci. 2010;52(3):1086–92.
16. Pekmez NÖ, Abaci E, Cinkilli K, Yağan A. Polybithiophene and its bilayers with polyaniline coatings on stainless steel by electropolymerization in aqueous medium. Prog Org Coat. 2009;65(4):462–8.
17. Liang C, Chen W, Huang N. Electrochemical characterization for polybithiophene film on porous oxide layer of 304 stainless steel formed by square wave passivation. Mater Corros. 2012;63:155–60.
18. Breslin CB, Fenelon AM, Conroy KG. Surface engineering: corrosion protection using conducting polymers. Mater Des. 2005;26(3):233–7.
19. Tüken T, Tansuğ G, Yazici B, Erbil M. Poly(N-methyl pyrrole) and its copolymer with pyrrole for mild steel protection. Surf Coat Technol. 2007;202(1):146–54.
20. Pekmez NÖ, Cinkilli K, Zeybek B. The electrochemical copolymerization of pyrrole and bithiophene on stainless steel in the presence of SDS in aqueous medium and its anticorrosive performance. Prog Org Coat. 2014;77(8):1277–87.
21. Alakhras F, Holze R. Redox thermodynamics, conductivity and Raman spectroscopy of electropolymerized furan–thiophene copolymers. Electrochim Acta. 2007;52(19):5896–906.
22. Liang L, Wei C, Ning X, Zhenggan X, Gi X. Electrochemical copolymerization of furan and 3-methyl thiophene. J Mater Sci. 2004;39(7):2395–8.
23. Maouche N, Nessark B. Electrochemical behavior of polyterthiophene-coated types 304 and 316 stainless steels and its corrosion performance. Corros Sci. 2008;64(4):315–24.
24. Troch-Nagels G, Winand R, Weymeersch A, Renard L. Electron conducting organic coating of mild steel by electropolymerization. J Appl Electrochem. 1992;22(8):756–64.
25. Nessakh B, Kotkowska-Machnik Z, Tedjar F. Electrochemical behaviour of furan, 2-methylfuran and 2,5-dimethylfuran in acetonitrile. J Electroanal Chem. 1990;296(1):263–8.
26. Lamiri L, Nessark B, Habelhames F, Sibous L. Electrochemical and spectroscopic characterization of poly (bithiophene + 2-methylfuran) copolymer. J Mol Struct. 2017;1143:282–7.
27. Yağan A, Pekmez NÖ, Yildiz A. Electrochemical synthesis of poly(N-methylaniline) on an iron electrode and its corrosion performance. Electrochim Acta. 2008;53(16):5242–51.
28. Srikanth AP, Nanjundan S, Rajendran N. Synthesis, characterization and corrosion protection properties of poly(N-(methacryloyloxymethyl) benzotriazole-co-glycidylmethacrylate) coatings on mild steel. Prog Org Coat. 2007;60(4):320–7.
29. Umoren SA, Li Y, Wang FH. Synergistic effect of iodide ion and polyacrylic acid on corrosion inhibition of iron in H_2SO_4 investigated by electrochemical techniques. Corros Sci. 2010;52(7):2422–9.
30. Mansfeld F. Use of electrochemical impedance spectroscopy for the study of corrosion protection by polymer coatings. J Appl Electrochem. 1995;25(3):187–202.
31. Rehim SSA, Hassan HH, Amin MA. Corrosion and corrosion inhibition of Al and some alloys in sulphate solutions containing halide ions investigated by an impedance technique. Appl Surf Sci. 2002;187(3–4):279–90.
32. Siva Kumar C, Shankar Rao V, Raja VS, Sharma AK, Mayanna SM. Corrosion behaviour of solar reflector coatings on AA 2024T3 – an electrochemical impedance spectroscopy study. Corros Sci. 2002;44(3):387–93.
33. Rehim SSA, Hassan HH, Amin MA. Corrosion inhibition study of pure Al and some of its alloys in 1.0 M HCl solution by impedance technique. Corros Sci. 2004;46(1):5–25.
34. Ashassi Sorkhabi H, Shabani B, Aligholipour B, Seifzadeh D. The effect of some Schiff bases on the corrosion of aluminum in hydrochloric acid solution. Appl Surf Sci. 2006;252(12):4039–47.

35. Zhou C, Lu X, Xin Z, Liu J, Zhang Y. Polybenzoxazine/SiO_2 nanocomposite coatings for corrosion protection of mild steel. Corros Sci. 2014;80:269–75.
36. Yuan X, Sun JC, Blanco M, Wang H, Zhang J, Wilkinson DP. AC impedance diagnosis of a 500W PEM fuel cell stack part I: stack impedance. J Power Sources. 2006;161(2):920–8.
37. Kumagai M, Myung ST, Ichikawa T, Yashiro H. Evaluation of polymer electrolyte membrane fuel cells by electrochemical impedance spectroscopy under different operation conditions and corrosion. J Power Sources. 2010;195(17):5501–7.
38. Sabouri M, Shahrabi T, Faridi HR, Hosseini MG. Polypyrrole and polypyrrole–tungstate electropolymerization coatings on carbon steel and evaluating their corrosion protection performance via electrochemical impedance spectroscopy. Prog Org Coat. 2009;64(4):429–34.
39. Walter GW. A review of impedance plot methods used for corrosion performance analysis of painted metals. Corros Sci. 1986;41(9):681–703.
40. Abaci S, Nessark B. Characterization and corrosion protection properties of composite material (PANI + TiO_2) coatings on A304 stainless steel. J Coat Technol Res. 2015;12(1):107–20.
41. Gnanakan SRP, Rajasekhar M, Subramania A. Synthesis of polythiophene nanoparticles by surfactant-assisted dilute polymerization method for high performance redox supercapacitors. Int J Electrochem Sci. 2009;4:1289–301.
42. Hotta S, Kohiki S. XPS and IR study of electrochemically or chemically redoped poly(3-methylthienylene) films. Synth Met. 1985;11(3):139–57.
43. Wei H, Scudiero L, Eilers H. Characterization of poly(3methyl thiophene) thin films prepared by modified chemical bath deposition. Appl Surf Sci. 2005;255:8593–7.
44. Zouaoui H, Abdi D, Bahloul A, Nessark B, Briotc E, Groult H, Mauger A, Julien CM. Electrosynthesis, characterization and photoconducting performance of ITO/polybithiophene –MnO_2 composite. Mater Sci Eng B. 2016;208:29–38.
45. Carrillo I, Sanchez de la Blanca E, Gonzales-Tejera MJ. Hernandez-Fuentes I. FTIR study of the influence of the deposition potential in the synthesis of polyfuran/perchlorate doped films. Chem Phys Lett. 1994;229(6):633–7.
46. Ai L, Liu Y, Zhang XY, Ouyang XH, Ge ZY. A facile and template-free method for preparation of polythiophene microspheres and their dispersion for waterborne corrosion protection coatings. Synth Met. 2014;191:41–6.
47. Alakhras F, Holze R. In situ UV–vis- and FT-IR-spectroscopy of electrochemically synthesized furan–thiophene copolymers. Synth Met. 2007;157(2–3):109–19.